Acta Crystallographica Section F
Structural Biology and Crystallization Communications
ISSN 1744-3091

Expression, purification and preliminary X-ray crystallographic analysis of Arf1-GDP in complex with dimeric p23 peptide

Peng Zheng,[a,b] Feng Gao,[a] Kai Deng,[c] Weimin Gong[a]* and Zhe Sun[a]*

[a]Laboratory of Noncoding RNA, Institute of Biophysics, Chinese Academy of Sciences, 15 Datun Road, Beijing 100101, People's Republic of China, [b]University of Chinese Academy of Sciences, Beijing 100039, People's Republic of China, and [c]Reproductive Medicine Research Center, Renmin Hospital, Hubei University of Medicine, Shiyan, Hubei 442000, People's Republic of China

Correspondence e-mail: wgong@ibp.ac.cn, zsun@moon.ibp.ac.cn

Received 4 June 2013
Accepted 31 August 2013

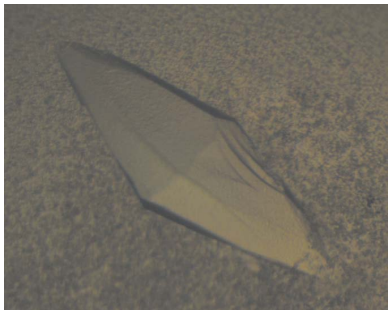

Arf1 is a member of the Ras superfamily and is involved in COPI vesicle formation. Arf1-GDP can interact with dimeric p23. Here, human Arf1 (residues 18–181) was cloned, expressed and purified in *Escherichia coli*. For crystallization, Arf1-GDP was mixed with dimeric p23 peptide in a 1:5 molar ratio. Crystals were obtained which diffracted to 2.7 Å resolution. The crystals belonged to space group $P6_122$, with unit-cell parameters $a = b = 80.6$, $c = 336.0$ Å, $\alpha = \beta = 90$, $\gamma = 120^\circ$. The asymmetric unit of the crystals contained two molecules, with a Matthews coefficient of 3.2 Å^3 Da^{-1} and a solvent content of 61.9%.

1. Introduction

The ADP-ribosylation factor (Arf) protein, a member of the Ras superfamily (Wennerberg *et al.*, 2005), is involved in the regulation of membrane traffic (D'Souza-Schorey & Chavrier, 2006). The cytoplasm of eukaryotic cells is spatially separated into distinct cellular compartments. Transport of proteins and lipids between these internal compartments is conducted by coated vesicles. There are three main coated vesicles: COPI, COPII and clathrin. COPI vesicles contribute to retrograde transport from the Golgi to the ER and transport within the Golgi. Coatomer, the coat protein of the COPI vesicle, is a 600 kDa complex made of seven subunits (α, β, β', γ, δ, ε and ζ). Arf1 plays a central role in recruitment of coatomer and formation of the COPI vesicles.

Arf protein was first identified as a cofactor for ADP-ribosylation of the α-subunit of heterotrimeric G proteins, Gs, catalyzed by cholera toxin *in vitro* (Kahn & Gilman, 1986). However, Arf protein is not involved in ADP-ribosylation of Gs *in vivo* (D'Souza-Schorey & Chavrier, 2006; Gillingham & Munro, 2007). There are six members in the mammalian Arf protein family (Arf1–6) with similar structural features. All Arf proteins have an amyristoylated N-terminal amphipathic helix and can cycle between the GDP-bound form (Arf-GDP) and the GTP-bound form (Arf-GTP). When GDP is displaced by GTP, the effector domain regions Switch 1 (residues 40–51 of Arf1) and Switch 2 (residues 68–81 of Arf1) open and the interswitch region between Switch 1 and 2 moves away from the nucleotide-binding site. This process pushes out the N-terminal amphipathic helix and promotes the membrane binding of this amphipathic helix (Nie *et al.*, 2003).

Arf1 is the best studied Arf family member and can recruit coatomer, AP1/3/4 (clathrin adaptor protein 1/3/4) and GGA (Golgi-localized, γ-adaptin ear-containing, Arf-binding proteins) to the Golgi apparatus (Popoff *et al.*, 2011). GEFs (guanine nucleotide-exchange factors) convert the inactive Arf-GDP to active Arf-GTP which anchors to the Golgi membrane (Bui *et al.*, 2009). Conversely, ArfGAPs (Arf GTPase-activating proteins) activate the Arf1 GTPase, which subsequently converts Arf1-GTP to Arf1-GDP and releases Arf1 from the Golgi membrane (Beck, Brügger *et al.*, 2011).

The process of COPI vesicle formation can be divided into six steps: membrane binding of Arf1, recruitment of coatomer, uptake of cargo, vesicle budding, vesicle scission and vesicle uncoating (Beck *et al.*, 2009). Membrane binding of Arf1 is the prerequisite for COPI vesicle formation, but it is unclear how Arf1 is recruited to the membrane.

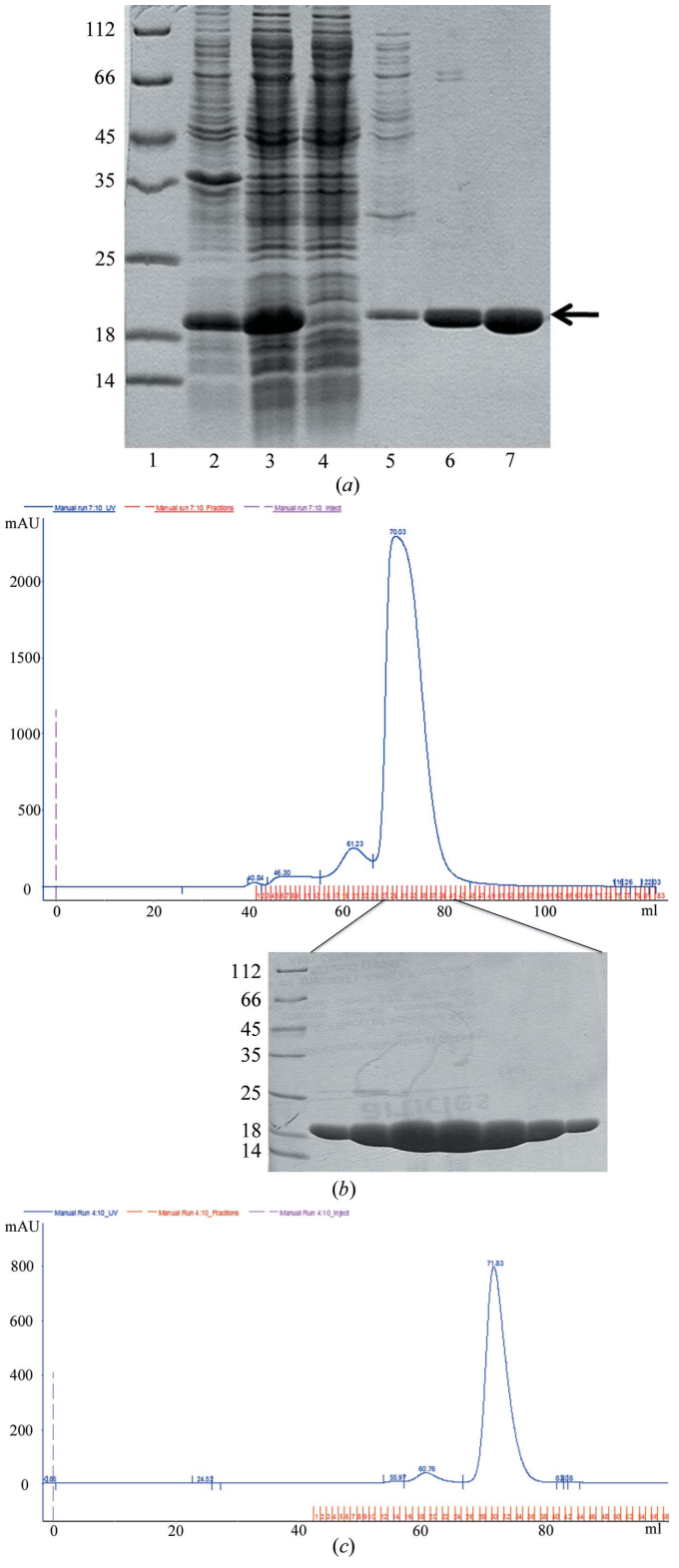

Figure 1
Purification of Arf1 and Arf1-GDP. (*a*) Results of nickel-affinity chromatography. Lane 1, molecular-mass markers (labelled on the left in kDa); lane 2, precipitate of the lysate; lane 3, supernatant of the lysate; lane 4, flowthrough; lanes 5, 6 and 7, elution fractions with 20, 50 and 200 m*M* imidazole, respectively. The arrow represents Arf1. The amount of Arf1 loaded in lane 7 of the gel was approximately 2.5 µg. (*b*) Purification of Arf1 by HiLoad 16/60 Superdex 75 pg and SDS–PAGE analysis of the major peak. (*c*) Purification of Arf1 after nucleotide exchange by HiLoad 16/60 Superdex 75 pg.

Arf1-GDP can interact with dimeric p23, a member of the type-I transmembrane protein p24 family. *In vitro* cross-linking assays and FRET (fluorescence resonance energy transfer) assays suggested that the C-terminal helix of Arf1-GDP can bind to the C-terminal tail of dimeric p23 (Gommel *et al.*, 2001; Majoul *et al.*, 2001). Recently, another study found that an Arf1 dimer is necessary for the scission of COPI vesicles (Beck, Prinz *et al.*, 2011). Given that p23 is important for the formation of COPI vesicles and Arf1 cannot interact with monomeric p23 (Popoff *et al.*, 2011), we hypothesize that p23 is potentially a key factor for Arf1-GDP recruitment and Arf1-GTP dimer formation. Since p23 is a transmembrane protein, most studies used chemosynthetic dimeric p23 peptide (the C-terminal tail of dimeric p23), disulfide-bridged *via* an additional cysteine at the N-terminus, to mimic the p23 protein. Here, we report the purification and crystallization of Arf1-GDP (residues 18–181) in complex with dimeric p23 peptide.

2. Materials and methods

2.1. Cloning, expression and purification

The gene encoding human Arf1 (residues 18–181; UniProt accession No. P84077) was amplified from a human brain cDNA library (Stratagene) using upstream primer 5′-GGAATTCCATATGATGCGCATCCTCATGGTGGGCCTGG-3′ and downstream primer 5′-CGCGGATCCTCACTTCTGGTTCCGGAGCTGATTGGACAG-3′ which contained *Nde*I and *Bam*HI restriction sites. The PCR products were digested with *Nde*I and *Bam*HI restriction enzymes (New England Biolabs) and then inserted into expression vector pET-15b (Novagen). The vector including the target gene was verified by DNA sequencing. The vector-derived residues MGSSHHHHHHSSGLVPRGSHM were fused at the N-terminus of Arf1.

The expression vector was transformed into *Escherichia coli* strain BL21 (DE3). The expression strain was cultured in 0.8 l LB medium containing 25 µg ml^{-1} kanamycin at 310 K until the OD_{600} reached 0.8. Recombinant protein was expressed by the addition of 0.1 m*M* IPTG (Sigma) and cell growth was continued for 6 h at 298 K.

The cells were harvested by centrifugation at 4000*g* for 40 min at 277 K and resuspended in lysis buffer (20 m*M* Tris–HCl pH 8.0, 150 m*M* NaCl). After sonication, the lysate was cleared by centrifugation at 38 900*g* for 30 min at 277 K. The supernatant was loaded onto a 2 ml pre-equilibrated Chelating Sepharose Fast Flow (GE Healthcare) column. The resin was washed with lysis buffer containing 20 and 50 m*M* imidazole, and the target protein was eluted at 200 m*M* imidazole. The volume of protein solution was reduced to approximately 1 ml by ultrafiltration for gel-filtration chromatography on a HiLoad 16/60 Superdex 75 pg column (GE Healthcare) at 277 K. Fractions containing Arf1 were then collected and concentrated for nucleotide exchange. As described previously (Seidel *et al.*, 2004), purified Arf1 was incubated with a 50-fold molar excess of GDP in phosphate buffer (10 m*M* KPO_4, 50 m*M* NaCl, 1 m*M* $MgCl_2$ pH 7.0) containing 1 m*M* EDTA overnight at room temperature. The nucleotide exchange was ended by the addition of 30 m*M* $MgCl_2$. The protein was then loaded onto a HiLoad 16/60 Superdex 75 pg column and eluted with phosphate buffer at room temperature to remove excess GDP, EDTA and $MgCl_2$. Fractions containing Arf1-GDP were collected and concentrated for crystallization. Protein concentration was determined using a Bio-Rad Protein Assay Kit.

2.2. Crystallization

For crystallization, Arf1-GDP (residues 18–181) was mixed with chemosynthetic dimeric p23 peptide [$(CLRRFFKAKKLIE)_2$, disulfide-bridged *via* an additional cysteine at the N-terminus; Fig. 2*a*] at a 1:5 molar ratio in phosphate buffer. The final concentration of Arf1-GDP was 10 mg ml^{-1}. After incubation for 1.5 h at room temperature, crystallization screening of the complex was set up with several commercial kits (Crystal Screen, Crystal Screen 2, Index and PEG/Ion; Hampton Research) at 289 K using the sitting-drop vapour-diffusion method. Protein solution (200 nl) in phosphate buffer was mixed with 200 nl reservoir solution and equilibrated against 30 µl reservoir solution using a Mosquito robot. Hexagonal bipyramid-shaped crystals were found in solution No. 69 of the Index kit [0.2 *M* ammonium sulfate, 0.1 *M* Tris pH 8.5, 25%(*w*/*v*) PEG 3350] after 8 d. The crystallization condition was optimized by varying the precipitant gradient, salt concentration, buffer pH and temperature (277 and 289 K) *via* the hanging-drop vapour-diffusion method. Changes of molar ratio of protein to peptide and volume ratio of protein solution to reservoir solution were also used for further optimization.

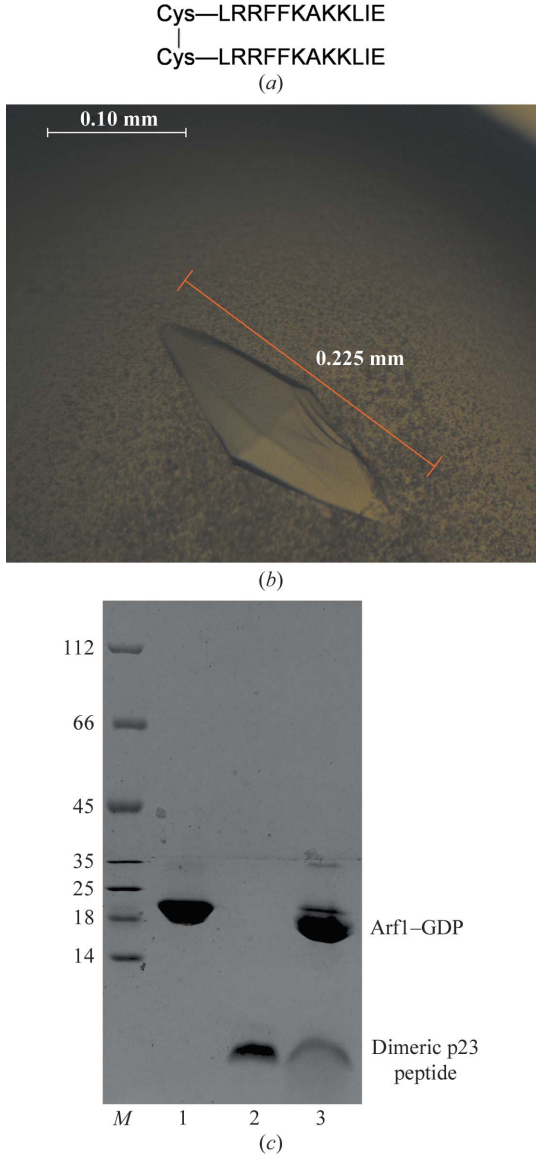

Figure 2
(*a*) Structure of dimeric p23 peptide. (*b*) Typical crystal of Arf1-GDP in complex with dimeric p23 peptide. (*c*) Analysis of crystals. Lane *M*, molecular-mass markers (labelled on the left in kDa); lane 1, Arf1-GDP; lane 2, dimeric p23 peptide; lane 3, crystals.

2.3. Data collection and X-ray diffraction analysis

Data collection was performed at 100 K using an ADSC Q315 detector on beamline BL17U of the Shanghai Synchrotron Radiation Facility (SSRF). Crystals were directly flash-cooled from the drops. 360 diffraction images were collected to 2.7 Å resolution with 1° oscillation and 1 s exposure time per image. The diffraction data were indexed, integrated, scaled and further processed using *HKL*-2000 (Otwinowski & Minor, 1997) and *CCP*4 (Winn *et al.*, 2011).

3. Results and discussion

The soluble protein bound to the nickel-affinity column following sonication and centrifugation was eluted by lysis buffer containing 200 m*M* imidazole. The result of SDS–PAGE showed that the purity of Arf1 was >95% and the molecular mass was approximately 20 kDa (Fig. 1*a*). According to the gel-filtration profiles, Arf1 isolated by nickel-affinity chromatography showed a major peak at 70.03 ml. After nucleotide exchange, Arf1 showed a major peak at 71.83 ml, which corresponds to an approximate molecular mass of 20 kDa on the basis of a standard curve (Figs. 1*b* and 1*c*). The small elution-volume shift of 1.8 ml (relative to the 120 ml bed volume) may be due to the difference in the running buffer. Finally, 15 mg purified protein was obtained from 0.8 l culture.

The best crystal diffracted to 2.7 Å resolution and was obtained from an optimized condition [0.2 *M* ammonium sulfate, 0.1 *M* Tris pH 8.0, 20%(*w*/*v*) PEG 3350] at 277 K after 5 d (Fig. 2*b*). The drop volume of crystals was 2 µl consisting of 1 µl protein solution and 1 µl reservoir solution. Tricine SDS–PAGE analysis of crystals which were previously washed five times in reservoir solution and finally

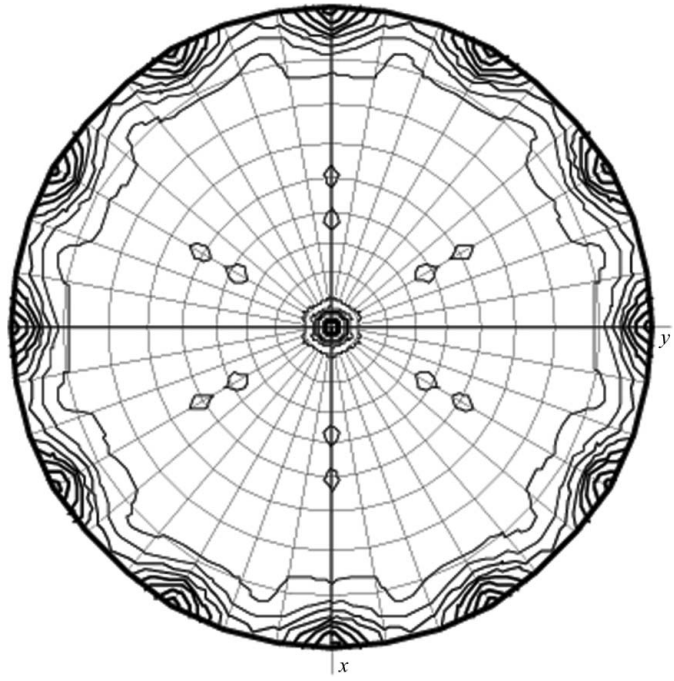

Figure 3
Self-rotation function for the crystal of Arf1-GDP in complex with dimeric p23 peptide.

Table 1
X-ray diffraction data and processing statistics.

Values in parentheses are for the outermost resolution shell.

Wavelength (Å)	0.97907
Unit-cell parameters (Å, °)	$a = b = 80.6$, $c = 336.0$, $\alpha = \beta = 90$, $\gamma = 120$
Space group	$P6_122$
Resolution (Å)	30.00–2.70 (3.80–2.70)
No. of reflections	169699
Unique reflections	18831
Completeness (%)	99.8 (100)
Average $I/\sigma(I)$	29.8 (3.3)
$R_{\rm merge}$† (%)	7.3 (54.8)
Multiplicity	9.0 (9.3)

† $R_{\rm merge} = \sum_{hkl}\sum_i |I_i(hkl) - \langle I(hkl)\rangle| / \sum_{hkl}\sum_i I_i(hkl)$, where $I_i(hkl)$ is the intensity of an individual measurement of a reflection and $\langle I(hkl)\rangle$ is the mean value for all equivalent measurements of this reflection.

dissolved in phosphate buffer (10 m*M* KPO_4, 50 m*M* NaCl, 1 m*M* $MgCl_2$ pH 7.0) showed that the crystals were indeed formed of the complex of Arf1-GDP and dimeric p23 peptide (Fig. 2*c*). A summary of the X-ray data statistics is shown in Table 1. The crystal belonged to space group $P6_122$, with unit-cell parameters $a = b = 80.6$, $c = 336.0$ Å, $\alpha = \beta = 90$, $\gamma = 120°$. The asymmetric unit of the crystal contained two molecules, with a Matthews coefficient of 3.2 $Å^3$ Da^{-1} and a solvent content of 61.9% (Matthews, 1968). The self-rotation function (SRF) calculated using *MOLREP* from the *CCP*4 suite (Winn *et al.*, 2011) is shown in Fig. 3. The resolution was limited to 5 Å and the radius of integration was 25 Å in the SRF. The result showed no noncrystallographic axes. There are no peaks higher than 15% of the height of the origin peak in the native Patterson.

We thank the staff of the Shanghai Synchrotron Radiation Facility for their assistance with data collection. This work was supported by the National Natural Science Foundation of China (grant No. 30870568).

References

Beck, R., Brügger, B. & Wieland, F. (2011). *Cell. Logist.* **1**, 52–54.
Beck, R., Prinz, S., Diestelkötter-Bachert, P., Röhling, S., Adolf, F., Hoehner, K., Welsch, S., Ronchi, P., Brügger, B., Briggs, J. A. & Wieland, F. (2011). *J. Cell Biol.* **194**, 765–777.
Beck, R., Rawet, M., Ravet, M., Wieland, F. T. & Cassel, D. (2009). *FEBS Lett.* **583**, 2701–2709.
Bui, Q. T., Golinelli-Cohen, M. P. & Jackson, C. L. (2009). *Mol. Genet. Genomics*, **282**, 329–350.
D'Souza-Schorey, C. & Chavrier, P. (2006). *Nature Rev. Mol. Cell Biol.* **7**, 347–358.
Gillingham, A. K. & Munro, S. (2007). *Annu. Rev. Cell Dev. Biol.* **23**, 579–611.
Gommel, D. U., Memon, A. R., Heiss, A., Lottspeich, F., Pfannstiel, J., Lechner, J., Reinhard, C., Helms, J. B., Nickel, W. & Wieland, F. T. (2001). *EMBO J.* **20**, 6751–6760.
Kahn, R. A. & Gilman, A. G. (1986). *J. Biol. Chem.* **261**, 7906–7911.
Majoul, I., Straub, M., Hell, S. W., Duden, R. & Söling, H.-D. (2001). *Dev. Cell*, **1**, 139–153.
Matthews, B. W. (1968). *J. Mol. Biol.* **33**, 491–497.
Nie, Z., Hirsch, D. S. & Randazzo, P. A. (2003). *Curr. Opin. Cell Biol.* **15**, 396–404.
Otwinowski, Z. & Minor, W. (1997). *Methods Enzymol.* **276**, 307–326.
Popoff, V., Adolf, F., Brügger, B. & Wieland, F. (2011). *Cold Spring Harb. Perspect. Biol.* **3**, a005231.
Seidel, R. D. III, Amor, J. C., Kahn, R. A. & Prestegard, J. H. (2004). *J. Biol. Chem.* **279**, 48307–48318.
Wennerberg, K., Rossman, K. L. & Der, C. J. (2005). *J. Cell Sci.* **118**, 843–846.
Winn, M. D. *et al.* (2011). *Acta Cryst.* D**67**, 235–242.